Pertanika J. Sci. & Technol. 27 (4): 2079 - 2107 (2019)

PERTANIKA JOURNALS

SCIENCE & TECHNOLOGY

Journal homepage: http://www.pertanika.upm.edu.my/

Optimization of Glass-beads Water Slurry flow Characteristics using Taguchi's Decision-making Technique coupled with Genetic Algorithm

Shofique Uddin Ahmed[1]*, Rajesh Arora[1] and Ranjana Arora[2]

[1]Department of Mechanical Engineering, Amity University, Haryana 122413, India
[2]Department of Renewable Energy, Amity University, Haryana 122413, India

ABSTRACT

This current study represents a numerical computational fluid dynamics (CFD) study of Glass beads-water slurry flow and aims for the optimization of various flow parameters adopting a new approach combining Taguchi's method and genetic algorithm (GA) for a smooth and better flow of the slurry. Three flow parameters viz. inlet mean velocity (V_m), volume fraction (C_{vf}) and particle size (D_p) with three levels were considered for the simulation and two responses vs. particle flow velocity (V_f) and pressure drop ($\frac{\Delta P}{L}$) were analysed to achieve a better understanding of the complex multiphase Glass-beads Water Slurry flow. Taguchi decision making technique and Genetic algorithm were exploited in order to optimize the particle flow velocity and pressure drop. A mathematical model was developed in order to forecast the responses analytically. Analysis of variance (ANOVA) was selected for finding the contribution of the selected flow parameters on particle flow velocity and pressure drop. The designed experiments were simulated numerically using analysis systems (ANSYS) software package by adopting Eulerian two-phase approach along with RNG K-ε model. Finally the optimized responses along with percentage reduction in pressure drop were reported and validated with the experimental data. This study optimized the pressure drop and particle flow velocity for three different input factors which would be helpful for the slurry-transporting industries, Oil and Gas industries and thermal power plants for optimal pipe design as well as to initiate a smooth slurry flow through horizontal pipeline.

Keywords: ANOVA, concentration distribution, genetic algorithm, pressure drop, regression analysis, slurry flow, Taguchi's method, velocity distribution

ARTICLE INFO

Article history:
Received: 20 September 2018
Accepted: 23 April 2019
Published: 21 October 2019

E-mail addresses:
uddinshofique1991@gmail.com (Shofique Uddin Ahmed)
rajesharora1219@gmail.com (Rajesh Arora)
ranjana1219@rediffmail.com (Ranjana Arora)
* Corresponding author

ISSN: 0128-7680
e-ISSN: 2231-8526

INTRODUCTION

Carrying solid materials through pipeline over a long distance has been imminent practice over the years in wide range of industries including oil and gas, manufacturing and production industries, food processing industries, city municipality, and pharmaceutical industries. Slurry flow is a process where solid particles are blended properly with fluid and is allowed to flow through pipelines over a long distance. The durability of this mode of solid material transport is that it is cost efficient as well as reduces air pollution, environmental hazards, and road traffic. Slurry flow is a complex multiphase flow problem. Flow parameters and flow patterns of slurry flow exhibit a complex behaviour and hence it is necessary to have detailed information about the slurry flow parameters and slurry flow patterns for a better understanding of the slurry flow process. Many classifications of slurry flow is available in the literature among which the most common classification includes homogenous flow, heterogeneous flow, stationary and moving bed flow and saltation flow regime. Among all these flow regime heterogeneous flow regime is the most occurring flow regime which shows a heterogeneous distribution of the solid particles within the fluid.

Computational fluid dynamics (CFD) is a sophisticated platform that allows the researchers to solve a wide range of complex flow problems at low cost and with greater ease. Many multiphase flow problems including slurry flow problems can be numerically analysed using this CFD technique which would have been very difficult to analyse experimentally. Hence the demand of CFD analysis is increasing day by day and researchers are adopting this cost efficient technique for their study. CFD provides exclusive idea about the variation of different flow variables inside the domain of the flow which plays a vital role in determining the behaviour of the flow process.

Taguchi's method is a sophisticated design technique for designing the experiments with least variance. It uses the concept of orthogonal array for arranging the experiments in proper order as well as allowing an optimal arrangement of the control parameters. Orthogonal Array produces a number of unbiased experimental settings with minimum number of experiments. Some logarithmic functions of the desired output or response are used in Taguchi's approach known as signal to noise ratio (S/N ratio) which acts as a key function in optimization process. Furthermore, Taguchi's technique aids to determine the desirable results and analysis of data. Generally, the larger the better, nominal the best and lower the better S/N ratios are used. S/N ratio considers the mean as well as the variability. S/N ratio is the ratio of mean aka signal to the standard deviation aka noise. Taguchi's technique allows an improvement of the productivity by reducing the influence of deviation without affecting the causes.

Analysis of Variance (ANOVA) is a statistical approach to developing impetus comparisons between two or more means; the yield results using this method can be tested to predict whenever powerful symbolic correlation exists between the variables. ANOVA

is an assemblage of statistical models and their combined measure where the inspected variance of a special variable is divided into components imputable to various provenances of variation. ANOVA is efficacious in confrontation of two, three or more means.

Researches in this area began at 3rd decades of 20th century. O'Brien (1933) and Rouse (1937) performed an experimental investigation on open channel slurry flow containing very low volume fraction and they studied the concentration distribution of fully suspended solid particles. Toda et al. (1973) conducted an experimental comprehensive study on two phase solid liquid slurry flow where they investigated the mean particle flow velocity for pipe bends, vertical and horizontal pipelines. They concluded that the particle velocities remained distributed in a wide range as well as the flow pattern of each particle exhibiting a different path. Turian and Yuan (1977) developed a pressure drop correlation for a multiphase slurry flow considering homogenous, heterogeneous, saltation flow and stationary bed flow. Their developed correlation showed an improvement in predicting pressure drop of the slurry flow. Oroskar and Turian (1980) developed a correlation implementing the energy used to suspend the particles to predict the critical velocity of slurry flow. Their proposed correlation was improved version of the previously available correlation for predicting the critical velocity. Roco and Shook (1983) developed a sequence of numerical equations for the prediction of velocity and concentration distribution of a quasi-uniform slurry flow considering different particle size. In their study explicit algorithm was used for determining numerical solutions of different flow patterns and the effects of solid particle size were determined. Doron et al. (1987) conducted an investigation of coarse particles slurry flow through horizontal tubes, they proposed a physical model to predict the pressure drop and flow patterns of the slurry flow and their proposed model was compared with their experimental results which showed a good consistency with the experimental results. Gillies et al. (1991) studied the slurry flow of gravel, sand and coarse coal particles and they proposed a mathematical model for predicting the head losses for these slurry flow. The contact load offering sliding friction at the wall of the pipe was found to be the objective function of their proposed model while this model was limited to the slurry flows containing less than 35% volume fraction of the particles. Gillies et al. (2004) conducted an experimental investigation of sand water slurry flow containing different particle size through horizontal pipeline having 103mm pipe diameter. In their study various flow variables such as *in situ* velocity and solid concentration and their effects on pressure drop were obtained and it was found that the friction loss showed a reduced effect at higher velocities. They also proposed a mathematical relation for predicting the friction loss at higher velocities and they used their proposed relation to rectify the model to determine slurry flow friction. Kaushal and Tomita (2007) studied the slurry flow of glass beads and water considering two particle sizes viz. 125µm and 440µm through a horizontal pipeline. They concentrated their study on determining the near wall lift of

the solid particles using γ-ray densitometer. From their study it was concluded that for the finer particles the highest concentration zone was near the pipe bottom while the highest concentration zone of coarser particles were established away from the base of the pipe. Lahiri and Ghanta (2010) developed a CFD generalized model for predicting the concentration distribution and pressure drop of a water- glass beads slurry flow adopting Eulerian two phase approach and RNG K-ε approach. The predicted pressure drop and concentration distributions were validated with the experimental data and were in an excellent consistency. Their proposed model showed an improvement for the prediction of flow parameters of slurry flow than the previously available models. Chandel et al. (2010) studied the rheological characteristics and pressure drop of a slurry flow containing fly ash and bottom ash above 50% concentration by weight using an experimental setup. Finally they determined the pressure gradient of slurry flow in straight pipes at high concentration using their rheological data and the pressure gradient was compared with the experimental data for the validation of their study. There are very few researches on optimization of flow problem using Taguchi's technique. Taguchi's technique helps us optimizing flow conditions selecting a set of optimal flow parameters that fits right for the optimum flow of the fluid through pipeline. Some of the researches in this field include the work of Wu et al. (2008); who reduced the micro bubble drag in a turbulent channel flow using Taguchi's robust design approach. In their study they looked into the impact of several controllable flow variables such as microbubble size, area of air injection and amount of air injected on microbubble drag reduction. From their study they found out that for optimum parametric conditions the effect of microbubble drag can be reduced upto 21.6%. Kotcioglu et al. (2013) conducted a comprehensive study for the selection of optimum design parameters in a rectangular duct heat exchanger using Taguchi's technique. They investigated the effect of various design variables such as pressure drop, flow velocity, Reynolds number, inclination angle of winglets, ratio of the winglets length to the duct channel length and ratio of the duct channel width to height for the performance parameter response of friction factor and Nusselt number.

This present study aims for the optimization of flow conditions for the smooth flow of water- glass beads slurry using a new approach combining Taguchi's method with Genetic Algorithm. Eulerian two phase approach along with RNG K-ε model was adopted for modelling the multiphase flow and turbulence phase of the flow respectively.

This present study represents CFD numerical analysis of glass beads-water slurry flow through a 54.9mm diameter and 4m length. In depth analysis of velocity profiles and concentration profile were carried out in order to achieve a better understanding of the complex multiphase slurry flow process. Three different flow parameters viz. inlet mean velocity, solid volume fraction and particle size were analyzed and their effects on pressure drop were determined. Experiments were designed in an unbiased fashion using Taguchi's L_9 Orthogonal Array. A logarithmic function S/N ratio was introduced

in order to optimize individually the particle flow velocity and pressure drop for three different flow conditions viz. inlet mean flow velocity, solid volumetric concentration and particle size. In addition a numerical model was developed using regression analysis to envisage the responses analytically. A new approach for multi-objective optimization was implemented exploiting the advantages of Genetic Algorithm and a specific combination of flow conditions was obtained which is capable of optimizing both the responses simultaneously. The contributions of these flow conditions on pressure drop and particle flow velocity were determined using Analysis of Variance statistical analysis tool. A range of particle sizes viz. 90µm, 125 µm and 150µm for inlet mean velocity of 3m/s, 4m/s and 5m/s with solid volume fraction of 30%, 40% and 50% were considered as the simulation parameters.(Flow Parameters). Finally the optimized responses obtained from GA analysis were compared with the simulated results as well as the simulated results of pressure drop were validated with the experimental results of pressure drop available in the literature of Kaushal and Tomita (2007). In addition the percentage reduction of pressure drop using this new strategy was reported in this present study.

METHODS

Model Description

Slurry flow problem is a multiphase flow problem. There are many mathematical models available foe modelling the multiphase flow in the commercial CFD software package ANSYS. Slurry flow consists of continuous liquid phase and discrete solid phase which cannot be considered as diffused dilute system. Here in this study Eulerian two-phase flow model had been selected for modelling the multiphase flow and RNG K-epsilon approach was selected for modelling the turbulence phase of the flow. The solid particles were assumed to be mono-dispersed. In other words the solid phase was assumed to behave like liquid because of its dispersed nature. One of the advantages of selecting Eulerian two-phase model is that the Eulerian model satisfies both the momentum and mass equation for the solid and fluid phase individually while at the same time the mixture model fails to predict the pressure drop correctly. Moreover, granular version of Eulerian two-phase model is preferred for modelling the slurry flow because unlike the non-granular version it takes into account of collision and friction among the solid particles which is an important factor that has to be considered while modelling the slurry flow.

Eulerian Two-Phase Model

This model comprises most complex equations of multiphase modelling in FLUENT software. In Eulerian model, the slurry is supposed to comprise solid and liquid phases. The concentrations of the two phases are assumed to be α_s and α_f for $\alpha_s + \alpha_f = 1$. In the present study, granular flows had been undertaken comprising fluid/solid intermixing

whose modelling could be achieved by appropriate constraints of interphase exchange and pressure coefficients. Moreover, the characteristics of the flow had been derived with the applications of kinetic theory. The various forces that act on a single solid particle are given as follows (Kaushal et al., 2012).

1. Static pressure gradient ΔP_s.
2. Inertial force caused by particles of solid pressure gradient ΔP_s.
3. Forces due to the difference in velocities of two phases, $K_{sf}\left(\vec{v}_s - \vec{v}_f\right)$
4. Viscous and body forces, $\nabla.\overline{\overline{\tau}}_f$ and $\rho\vec{g}$, where $\overline{\overline{\tau}}_f$ represents the stress tensor of fluid, ρ denotes the mass density and g is gravitational acceleration.
5. Lift/virtual mass forces. The coefficient of virtual mass/ lift forces, C_L/C_{vm} are assumed to be 0.5.
6. The particles in the analysis are assumed to be fluid in nature.

In this paper, an efficient Eulerian-Eulerian multi-phase model is adopted for numerical simulation. The following governing equations are used for the turbulent flow of fly ash particles in the Newtonian fluid.

Governing Equations

Continuity Equation

$$\nabla.(\alpha_t \rho_t \vec{v}_t) = 0, \text{ } t \text{ being either } \textit{solid} \text{ or } \textit{fluid.} \quad (1)$$

Momentum equation for fluid phase

$$\nabla.\alpha_f \rho_f \vec{v}_f \vec{v}_f = -\alpha_f \nabla P + \nabla.\bar{\bar{\tau}}_f + \alpha_f \rho_f \vec{g} + K_{sf}\left(\vec{v}_s - \vec{v}_f\right) + C_{vm}\alpha_f \rho_f \left(\vec{v}_s \nabla \vec{v}_s - \vec{v}_f \nabla \vec{v}_f\right)$$
$$+ C_L \alpha_s \rho_f (\vec{v}_f - \vec{v}_s) \times \nabla \times \vec{v}_f \quad (2)$$

Momentum equation for solid phase

$$\nabla.\alpha_s \rho_s \vec{v}_s \vec{v}_s = -\alpha_s \nabla P - \nabla P_s + \nabla.\bar{\bar{\tau}}_s + \alpha_s \rho_f \vec{g} + K_{sf}\left(\vec{v}_f - \vec{v}_s\right) + C_{vm}\alpha_s \rho_f \left(\vec{v}_f \nabla \vec{v}_f - \vec{v}_s \nabla \vec{v}_s\right)$$
$$+ C_L \alpha_s \rho_f (\vec{v}_s - \vec{v}_f) \times \nabla \times \vec{v}_f \quad (3)$$

$\bar{\bar{\tau}}_f$ and $\bar{\bar{\tau}}_s$ being the stress tensor for the fluid and solid phase respectively.

$$\bar{\bar{\tau}}_f = \alpha_f \mu_f \left(\nabla \vec{v}_f + \nabla \vec{v}_f^{tr}\right) \quad (4)$$

$$\bar{\bar{\tau}}_s = \alpha_s \mu_s (\nabla \vec{v}_s + \nabla \vec{v}_s^{tr}) + \alpha_s (\lambda_3 - \frac{2}{3}\mu_s) \nabla \vec{v}_s \bar{\bar{I}} \quad (5)$$

The bulk viscosity of solid can be donated by λ_s and is represented as

$$\lambda_s = \frac{4}{3}\alpha_s \rho_s d_s g_{o,ss}(1+e_{ss})\left(\frac{\Theta_s}{\pi}\right)^{\frac{1}{2}} \quad (6)$$

The turbulence model is solved by using RNG K-eplison approach with other additional conditions causing interfacial turbulent momentum transfer. The Reynolds stress tensor for the fluid phase is given by

$$\bar{\bar{\tau}}_{t,f} = -\frac{2}{3}\left(\rho_f k_f + \mu_{t,f}\nabla\vec{v}_f\right)\bar{\bar{I}} + \mu_{t,f}\left(\nabla\vec{v}_f + \nabla\vec{v}_f^{tr}\right) \quad (7)$$

Here $\mu_{t,f}$ is the fluid viscosity corresponding to the turbulence. An analytical differential interrelationship for turbulent viscosity is provided with RNG K-epsilon approach for modelling the flow at lower Reynolds number. However, for the sake of the present study which is based on high Reynolds number the analytical correlation converts to

$$\mu_{t,f} = \rho_f C_\mu \frac{k_f^2}{\varepsilon_f} \text{ with } C_\mu = 0.09 \quad (8)$$

The prediction of turbulent kinetic energy k_f and turbulent energy dissipation rate ε_f is by Standard K-epsilon method and RNG K-epsilon method is almost alike. Standard and RNG K-epsilon approach differ in such a fashion that RNG K-epsilon approach contains a supplementary expression in the epsilon equation

$$R_\varepsilon = \frac{C_\mu \rho \eta^3 (1-\eta/\eta_0)\varepsilon^2}{(1+\beta\eta^3)k} \quad (9)$$

Where $\eta = Sk/\varepsilon$, η_0 = 4.38, β = 0.012, the constant parameters are taken as $C_{\mu m}$= 0.0845, $C_{1\varepsilon}$= 1.42, $C_{2\varepsilon}$= 1.68, $C_{3\varepsilon=1.3}$ σ_k= 0.75, σ_ε = 1.2

Solution Strategy

In this current study the Navier-Stokes governing equations along with their closure parameters are solved using ANSYS FLUENT 14.0. Momentum and mass equations are solved by control volume finite difference approach. Turbulent kinetic energy, momentum equation and turbulent dissipation rate are discretized using second order upwind scheme while for discretizing the volume fraction first order upwind scheme is used in this study. For pressure and velocity coupling phase coupled SIMPLE algorithm is selected. Convergence of problem depends on the scaled residual. For this flow problem the residuals contains continuity, X-velocity, Y- velocity, Z-velocity for both the phases; k and ε for phase 1 and volume fraction for phase 2 which need to be converged at some specific region. Application of these schemes confirmed better stability, accuracy and convergence of the flow problem. Moreover decreasing the value of under relaxation factors ensures better convergence of

the problem. URF (under relaxation factor) for volume fraction has been reduced to 0.3 from 0.5 and for momentum it has been reduced from 0.7 to 0.5.

Geometry and Mesh

A circular pipe of 54.9mm diameter and 4m length had been modelled in ANSYS WORKBENCH design modular. A non-uniform structured mesh with hexa core elements was selected for meshing the whole computational domain as shown in Figure 1. Seven layers of inflations were selected with 0.005mm size and growth rate 1.2 for refining the mesh near the wall of the pipe. This is important for achieving more precise results near the wall boundary.

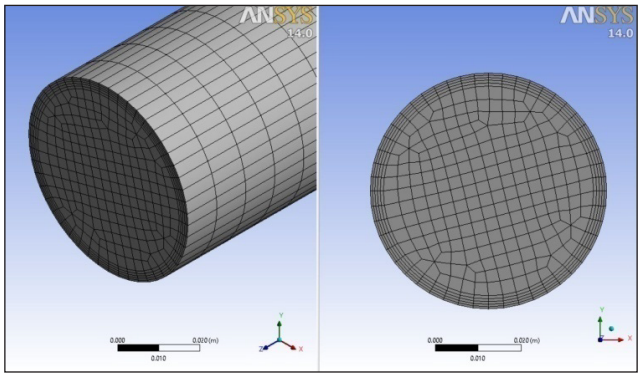

Figure 1. 3D and 2D view of the mesh selected for this study.

Grid Independency Test

Selection of proper grid size is highly recommended in most of the CFD numerical analysis problems. It provides better and enhanced simulation results. In this study, five mesh with different numbers of elements viz 0.95 Lakhs, 1.50 Lakhs, 2 Lakhs, 3.1 Lakhs and 3.89 Lakhs were introduced and simulations were conducted imposing same boundary conditions(V = 5m/s, C_{vf} = 0.3) for each of the mesh as shown in Figure 2. It had been found from the velocity plots for each of the mesh, that the velocity distribution of mesh having 2 Lakhs elements and 3.10 Lakhs elements were super imposing, hence the mesh with 2 Lakhs elements had been considered as the optimal mesh in this present study.

Boundary Conditions

Three boundary conditions had been imposed to the computational flow domain namely inlet boundary, wall boundary and outlet boundary. At inlet boundary, inlet mean flow velocity and solid volume fraction was introduced, while at wall boundary No-slip boundary conditions had been imposed. The outlet boundary had been treated as pressure outlet for solid as well as fluid phase.

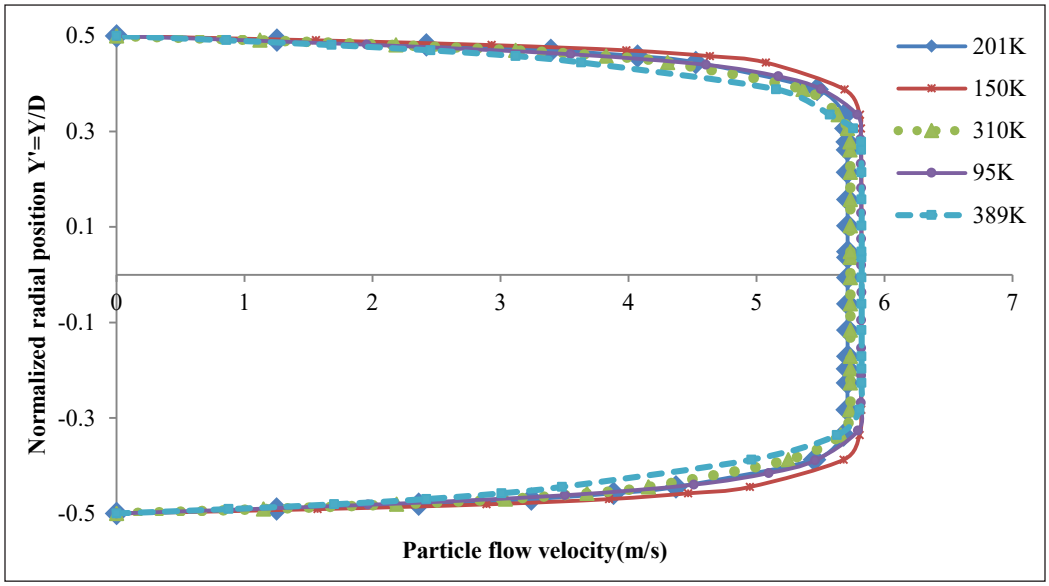

Figure 2. Plot of Grid Independency test

RESULTS AND DISCUSSION

Velocity Distribution

Figures 3 to 6 show the distribution of particle flow velocity at various volume fraction and particle size along the cross section of the pipe. The velocity contours are obtained at 3.9m length of the pipe from the inlet.

Figures 3 and 4 illustrate the particle flow velocity distribution of 90µm particle size and 30% solid volume fraction for different inlet mean velocity. From these figures it can be observed that at low inlet mean velocity (Figure 3a) the particle flow velocity distribution was asymmetrical at the base of the pipe, but this asymmetric nature reduced as the inlet mean velocity increased (Figure 3c).This is because of the reason that as the

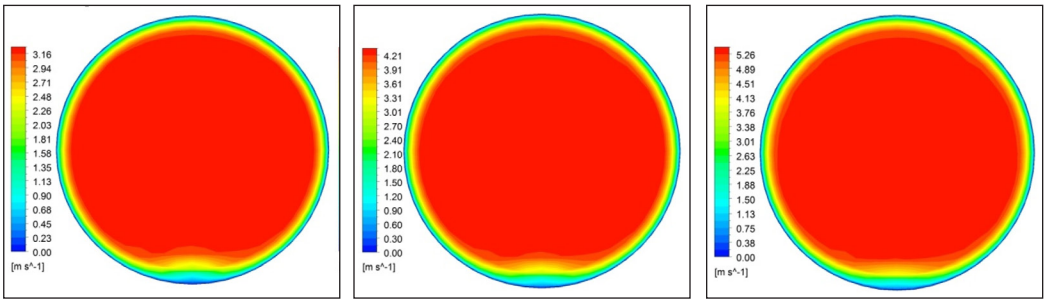

(a) (b) (c)

Figure 3. Particle flow velocity distribution (V_f) of 90µm particle size and 30% solid volume fraction (C_{vf}) for different inlet mean velocity (V_m): (a) V=3m/s; (b) V=4m/s; (c) V=5m/s

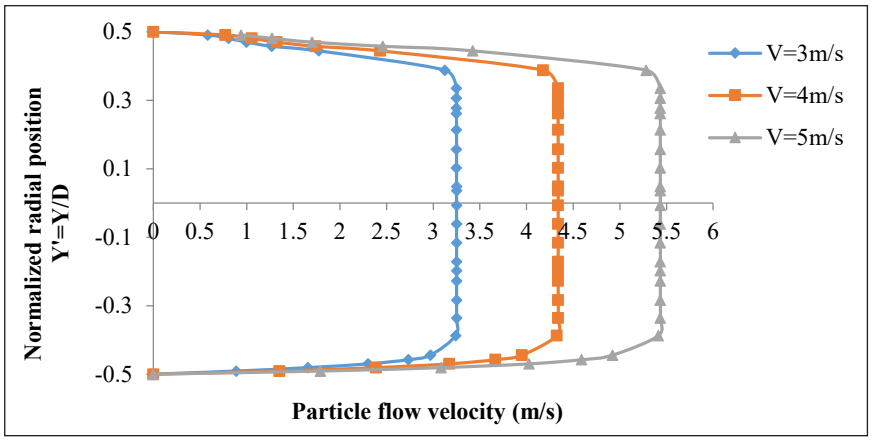

Figure 4. Plot of Particle flow velocity distribution (V_f) of 90µm particle size and 30% solid volume fraction (C_{vf}) for different inlet mean velocity (V_m)

inlet velocity becomes high, there is an increase in the flow turbulence, providing a perfect blending for the solid particles with the fluid. As a result, the solid particles became more distributed throughout the entire fluid region and hence, lesser number of solid particles could accumulate at the base of the pipe. Hence, the velocity distribution becomes more symmetrical at high inlet velocity (say V_m = 5m/s).

Figures 5 and 6 show the effect of solid volume fraction and particle size on particle flow velocity at a given inlet mean velocity. It can be noticed from Figure 6 that the velocity distribution was influenced by the solid particle size. As a result, the velocity profile became more distorted as the particles became larger in size from 90µm to 150µm. This may be the result of gathering of coarse particles at the base of the pipeline due to gravitational effect. Moreover, the degree of distortion of particle velocity is influenced by the solid volume fraction. For instance, at low volume fraction (C_{vf} = 0.3), the velocity profile is

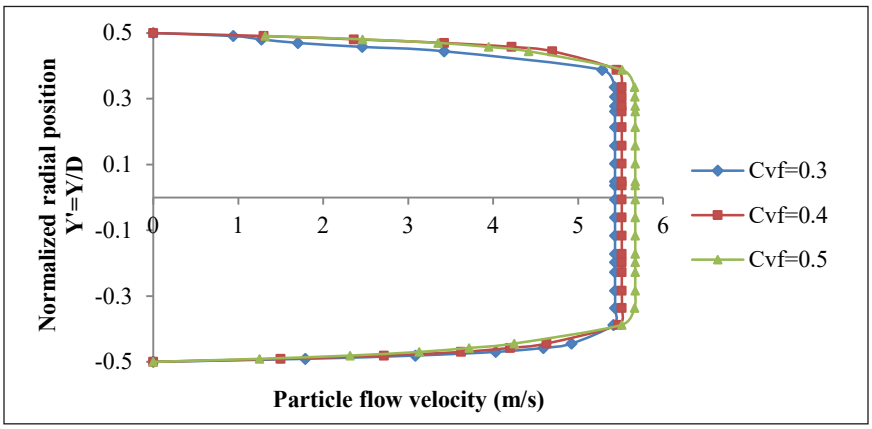

Figure 5. Plot of particle flow velocity distribution (V_f) at constant inlet mean velocity (V_m = 5 m/s) for different solid volume fraction (C_{vf}= 0.3, 0.4 and 0.5)

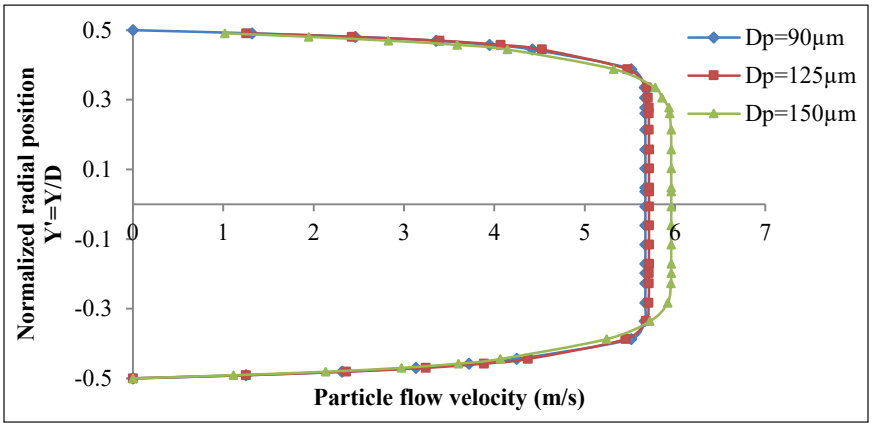

Figure 6. Plot of particle flow velocity distribution (V_s) at constant inlet mean velocity (V_m = 5m/s) at constant volume fraction (C_{vf} = 0.5) for different particle size D_p)

less distorted as well as the velocity is lower than that of high-volume fraction (C_{vf} = 0.5) (Figure 5). This might be the effect of increased turbulence energy at high volume fraction. In addition to this, it can be observed that the particle flow velocity decreases with the decrease in particle size for each solid volume fraction. As a result, smaller particles show more buoyancy effect which leads to symmetrical distribution and better blending of particles with the fluid that causes smoother flow of solid particles throughout the pipeline.

From this section it can be summarized that for obtaining maximum particle flow velocity a slurry flow with higher inlet mean velocity and high solid volume fraction as well as larger particle size is highly recommended.

Concentration Distribution

Figures 7 to 9 show the distribution of local concentration of solid particles along the vertical centreline of the pipe outlet, $Y' = Y / D$, Y is the vertical distance of the pipe from top to bottom and D is diameter of the pipe.

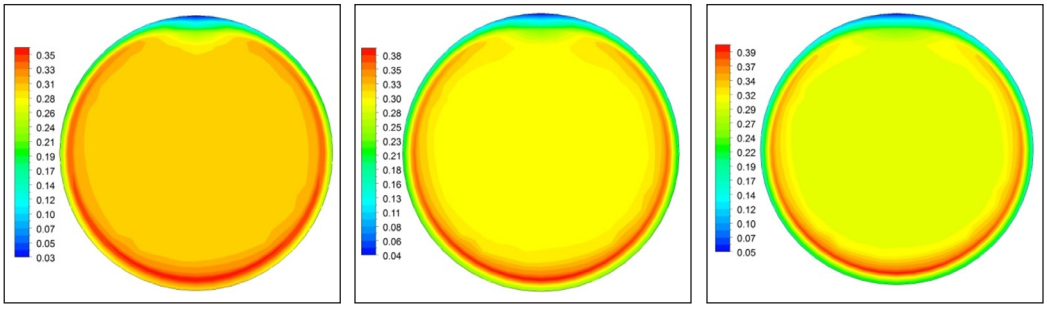

(a) (b) (c)

Figure 7. Concentration distribution of 90µm particle size and 30% solid volume fraction (C_{vf}) for different inlet mean velocity (V_m): (a) V=3m/s; (b) V=4m/s; (c) V=5m/s

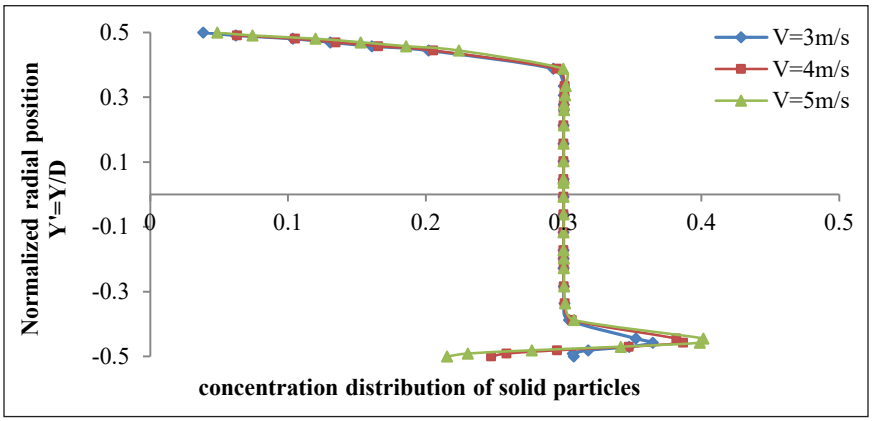

Figure 8. Plot of Concentration distribution of 90µm particle size and 30% solid volume fraction (C_{vf}) for different inlet mean velocity (V_m)

From Figures 7 to 8, it is noteworthy that the distribution of solid particles was asymmetrical across the vertical centreline of the pipe outlet, the high distribution zone being at the lower half of the pipe, where most of the solid particles seemed to accumulate at the base of the pipe. For low inlet mean velocity, the particles were accumulated at the base of the pipe (Figure 7a), but as the inlet mean velocity increased the solid particles became more buoyant and suspended in the fluid (Figure 7c) thereby providing their proper mixing with the fluid and ensuring a smooth slurry flow. This is because of the fact that when the inlet velocity increases, there is an increase in turbulence in the flow which is accountable for the mixing of solid particles with the fluid. Hence, at high inlet velocity (say 5m/s) the solid particles remains suspended in the fluid rather than settling down at the base of the pipe and hence, the concentration distribution becomes more distributed and symmetrical.

From Figure 9 it can be noticed that the distribution of solid particles was more homogenous when the particle size was small. It is also seen that the smallest particles (D_p= 90µm) being most buoyant as well as the distribution of particles in the fluid phase was homogenous. The particle concentration zone was distributed symmetrically over the vertical cross section at pipe outlet. However, as soon as the particle size became larger (from 90µm to 150µm) the concentration zone was shifted towards the lower portion of the pipe i.e. the base of the pipe cross section because of the gravitational effect, as a result the concentration zone became asymmetrical. As a result, the larger particles concentrate at the base of the pipe forming a stationary bed and refuse to travel further along with the fluid to the exit of the pipe. Further, as the particles become larger the thickness of the bed tends to increase and thereby reducing the effective flow area, which leads to poor productivity. The simulated results showed that the maximum concentration at the pipe bottom for 90µm is 0.35 whereas for 150µm particles it goes up to 0.41.

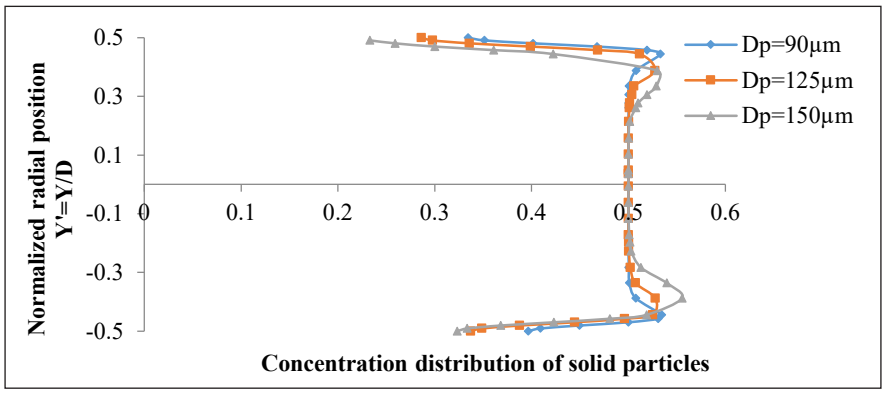

Figure 9. Plot of concentration distribution of solid particles at constant inlet mean velocity (V_m) and constant solid volume fraction (C_{vf}) for different particle size

Influence of Inlet Mean Velocity on Pressure Drop

Figure 10 shows the plot of effect of inlet mean velocity on pressure drop at different solid volume fraction for 125µm particle size.

From Figure 10 it is noteworthy that the pressure drop rose with the increase in inlet flow velocity. This is the result of increase in turbulence in the flow at high velocities which led to an increase in pressure drop. Moreover, as the volume fraction became high, the rate of rise in pressure drop also increased.

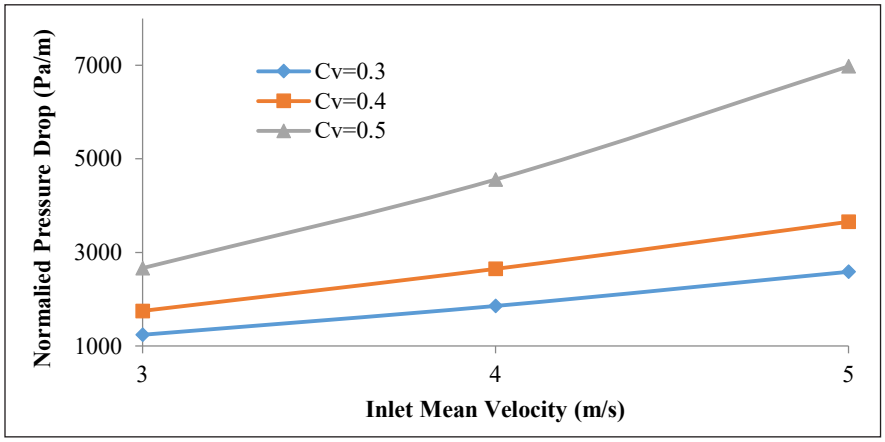

Figure 10. Plot of the effect of inlet mean velocity on pressure drop

Effect of Particle Size on Pressure Drop

Figure 11 shows the effect of particle size on pressure drop at different inlet mean velocity. It is noteworthy that there is a surge in pressure drop as the particles become larger. This happens because the larger particles tended to concentrate at the pipe bottom

due to gravitational effect and thereby reducing the effective flow area which caused an increase in turbulence of the flow. The increase in rate of pressure drop at higher inlet mean velocities can also be observed from the figure. Moreover, it can be noticed that the solid volume fraction plays an important role during the change in pressure drop. The degree of rise in pressure drop is low for lower volume fraction because at low volume fraction the turbulence is lower but when the solid volume fraction increases there is an increase in turbulence and hence, the pressure drop increases abruptly.

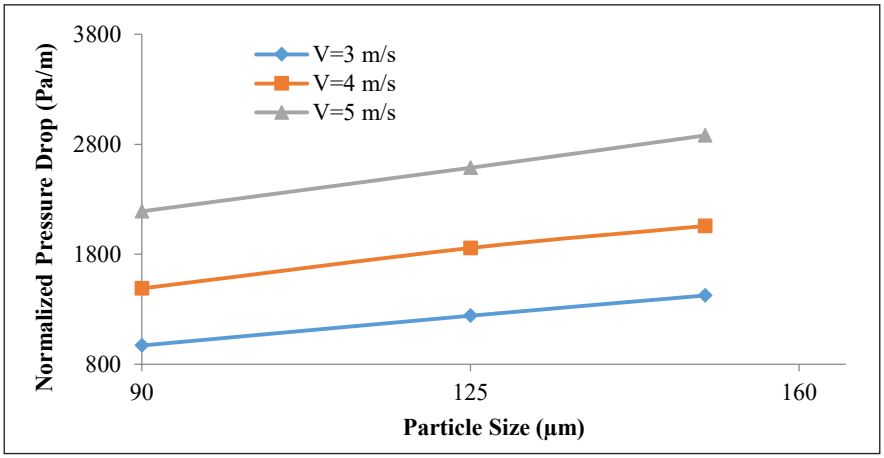

Figure 11. Plots of effect of particle size on pressure drop at constant volume fraction (C_{vf}= 0.3) for different inlet mean velocity

Effect of Volume Fraction on Pressure Drop

From Figure 12 it can be noticed that the pressure drop arose at higher volume fraction. At lower volume fraction (0.3) the pressure drop was lower and it rose as the volume fraction increased to 0.5. This is because of the fact that the turbulence of the flow becomes higher

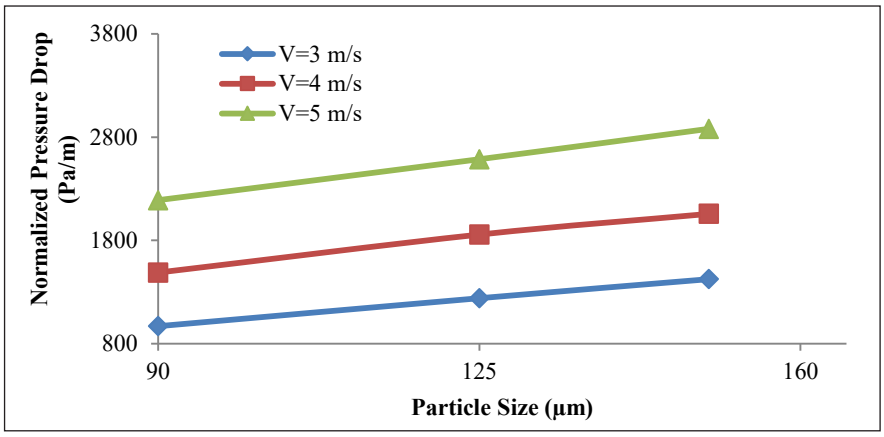

Figure 12. Effect of volume fraction (C_{vf}) on pressure drop at different particle size

with the increase in volume fraction thereby increasing the pressure drop. Furthermore, it was observed that with larger particle size the pressure drop also increased.

Prediction of Optimum Slurry Flow Conditions using Taguchi's Decision Making Technique

The aim of this section is to determine optimum flow condition for the maximum particle flow velocity and nominal pressure drop. When the particle flow velocity is high, the solid particles flow in a faster rate as well as the suspension of the solid particles also increases providing a complete mixing of solid particles with the fluid and ensuring a smooth slurry flow with minimal bed formation at the base of the pipe (Chandel et al., 2010). This will eventually increase the productivity. Furthermore, when the pressure drop is higher, there is an increase in frictional loss since pressure drop is directly proportional to frictional loss. Moreover, when the pressure drop is less, due to low turbulence, the solid particles tend to accumulate at the pipe bottom, hence creating a bed which reduces the effective flow area and hence productivity. Therefore, a nominal pressure drop is required for the smooth flow of slurry through the pipeline.

To determine the optimal flow condition Taguchi's L_9 orthogonal array was selected and inlet mean velocity, solid volume fraction and particle size were considered as input parameters (factors) of L_9 orthogonal array considering three levels for each of the factor. Since the desired output was maximum particle flow velocity, larger the better S/N ratio had been selected and can be represented by the following mathematical equation

$$S/N = -10 \times \log_{10} [(1/n) \times \text{Sum} (1/y_i^2)] \quad (10)$$

Here, n=Number of response and Y_i= particle flow velocity

Since Nominal pressure drop was the desired output, nominal is the best S/N ratio had been selected and can be represented by the following mathematical equation

$$\text{Eta} = 10 \times \log_{10} (\text{Mean}^2/\text{Variance}) \quad (11)$$

Table 1 represents selected factor and their levels where as L_9 orthogonal array of Taguchi's robust design approach is shown in Table 2.

Table 1
Selected factor and their levels

Factors	Level 1	Level 2	Level 3
Inlet mean velocity (V_m) m/s	3	4	5
Solid volume fraction (C_{vf})	0.3	0.4	0.5
Particle size (D_p) µm	90	125	150

Table 2
L_9 orthogonal array of Taguchi's robust design approach

Run	Factors		
	A	B	C
1	1	1	1
2	1	2	2
3	1	3	3
4	2	1	2
5	2	2	3
6	2	3	1
7	3	1	3
8	3	2	1
9	3	3	2

Design of Experiments

Table 3 shows the assignment table of L_9 orthogonal array adopted in this study whereas Response (Particle flow velocity) obtained from CFD simulated results and their corresponding S/N ratio is shown in Table 4.

Table 3
Design matrix of the experiments using Taguchi's L_9 orthogonal array

Experiment no.	Column		
	V_m (m/s)	C_{vf}	D_p (µm)
1	3	0.3	90
2	3	0.4	125
3	3	0.5	150
4	4	0.3	125
5	4	0.4	150
6	4	0.5	90
7	5	0.3	150
8	5	0.4	90
9	5	0.5	125

Results of particle flow velocity (response) and Pressure drop obtained from CFD simulation of the above experiments are tabulated in Table 4.

The following Figures 13 and 14, obtained from Minitab software shows the plots of mean S/N ratio vs. the flow parameters i.e. inlet mixture velocity, solid volume fraction and particle size.

For the analysis of the results obtained from the experiments designed by Taguchi's approach, S/N ratio analysis is used. Since "Larger the better" S/N ratio was selected for the analysis of particle flow velocity hence the highest mean of S/N ratio in Figure 14

Table 4
Response (Particle flow velocity and Pressure drop) obtained from CFD simulated results and their corresponding S/N ratio

Experiment no.	Particle flow velocity (m/s)	Pressure drop (Pa/m)	S/N ratio for particle flow velocity	Mean for pressure drop
1	3.249	969.16	10.2350	969.16
2	3.418	1750.285	10.6754	1750.28
3	3.617	3092.183	11.1670	3092.18
4	4.403	1856.318	12.8750	1856.32
5	4.2134	2973.085	13.2438	2973.08
6	4.543	3573.058	13.1469	3573.06
7	5.511	2880.548	14.8246	2880.55
8	5.513	3046.658	14.8278	3046.66
9	5.712	6974.703	15.1358	6974.70

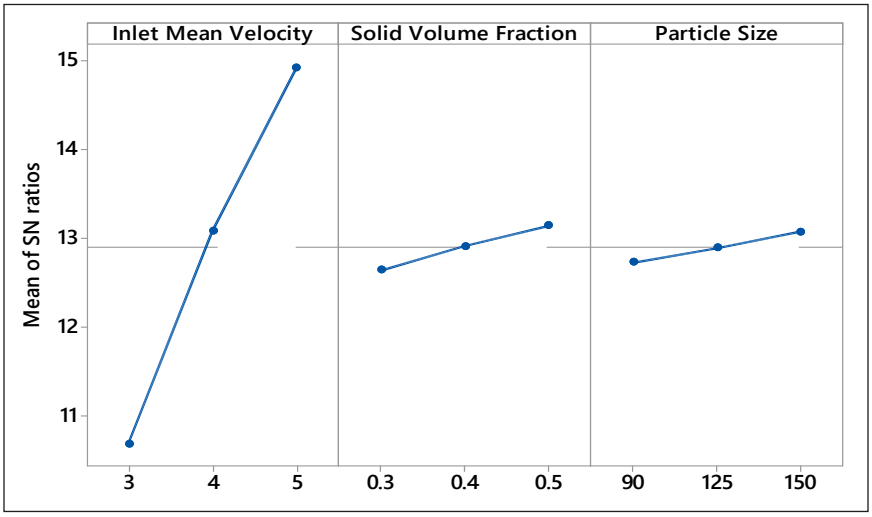

Figure 13. Influence of different flow parameters at different levels on S/N ratio of maximum particle flow velocity.

corresponds to the optimal level of input variables. In other words from the S/N analysis for maximum particle velocity the following conclusions can be drawn

- The inlet mean velocity should be 5m/s
- Solid volume fraction should be 0.5
- Particle size should be 150 µm

ANOVA Results

ANOVA was performed for determining the contributions of the flow parameters on particle flow velocity.

Table 5
Analysis of Variance results for particle flow velocity

Source	DOF	Seq SS	Contribution	Adj SS	Adj MS	F-Value	P-Value
Inlet mean velocity	2	6.93825	98.38%	6.93825	3.46913	5628.65	0.000
Solid volume fraction	2	0.08379	1.19%	0.08379	0.04190	67.98	0.014
Particle size	2	0.02907	0.41%	0.02907	0.01453	23.58	0.041
Error	2	0.00123	0.02%	0.00123	0.00062		
Total	8	7.05234	100.00%				

Table 5 shows that the highest contribution on particle flow velocity is inlet mean velocity (98.38%) followed by solid volume fraction (1.19%) and particle size (0.02%).

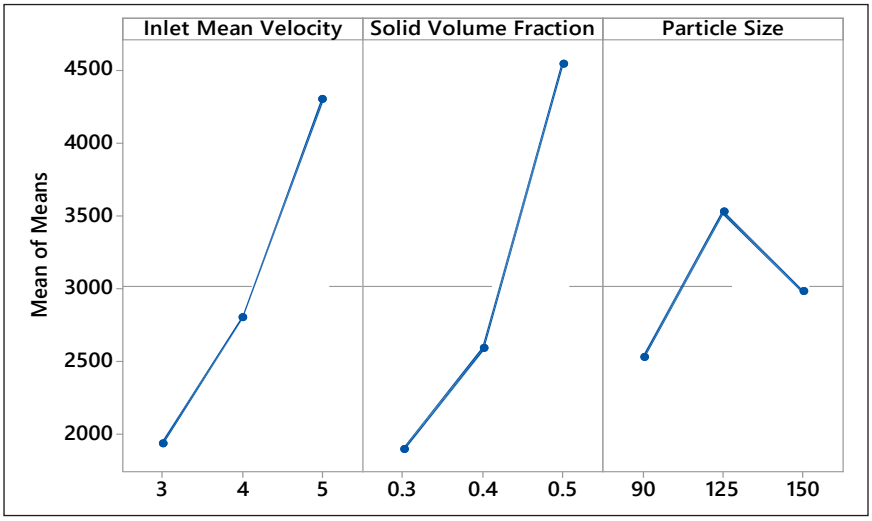

Figure 14. Influence of various flow parameters at different levels on Mean of nominal pressure drop.

Since "Nominal is best" S/N ratio has been adopted for the analysis of pressure drop, hence the nominal value (middle value) of the plot (Figure 15) represents the optimal level of the input parameters. In other words, the S/N analysis for nominal pressure drop shows the following results:

- Inlet mean velocity should be 4m/s
- Solid volume fraction should be 0.4
- Particle size should be 125 µm.

ANOVA was performed to determine the contributions of flow parameters on pressure drop.

From Table 6, it can be noticed the highest contribution on pressure drop was of solid volume fraction (48.41%) followed by inlet mean velocity (39.6%) and particle size (5.31%).

Table 6
Analysis of Variance results for pressure drop

Source	DF	Seq SS	Contribution	Adj SS	Adj MS	F-Value	P-Value
Inlet Mean Velocity	2	8581057	37.08%	8581057	4290528	4.84	0.171
Solid Volume Fraction	2	11295895	48.81%	11295895	5647948	6.38	0.136
Particle Size	2	1496750	6.47%	1496750	748375	0.85	0.542
Error	2	1771234	7.65%	1771234	885617		
Total	8	23144936	100.00%				

The optimal combination of input variables obtained from S/N ratio analysis is enlisted in Table 7.

Table 7
Optimal Parameter combinations obtained from S/N ratio analysis for both the responses.

	Optimal Parameter combination			Responses	
Combinations	Inlet Mean Velocity (m/s)	Solid Volume Fraction	Particle size (μm)	Particle flow velocity	Pressure drop
I	**5**	**5**	**150**	**5.9581**	6832.87
II	**4**	**4**	**150**	4.21	**2973.085**

Note. Bold values represent the optimal parameters and optimal responses

From Table 7 it can be observed that both the responses cannot be optimized simultaneously adopting Taguchi's S/N ratio analysis. Hence to overcome this problem a more sophisticated analysis is required. In this study to optimize both the responses Genetic Algorithm has been adopted.

Development of Numerical Models

Regression Analysis. Linear Regression model has been adopted to develop a correlation between multiple variables when there is a correlation among the dependent variables and independent variables. In this study V_m and $\frac{\Delta P}{L}$ are considered as dependent variables while V_m, C_{vf} and D_p are considered as independent variables. The general model equation for multivariable linear regressions is:

$$y = \beta_0 + \beta_1 x_1 + \beta_2 x_2 + \cdots \ldots \ldots \ldots \ldots \ldots + \beta_p x_p + \varepsilon \qquad (11)$$

Where x is the independent variable and y is the dependent variable. β's are coefficient (regression parameters) and ε is the residue.

From this general model equation mathematical equations are developed for prediction of Particle flow velocity and pressure drop for various control parameters.

The Regression Equation for Particle flow velocity V_f and pressure drop $\frac{\Delta P}{L}$ can be given as follows

$$V_f = 1.07533V_m + 1.1817C_{vf} + 0.002307D_p - 0.5481 \quad (12)$$

With $R^2 = 99.98\%$

And

$$\frac{\Delta P}{L} = 1182V_m + 13223C_{vf} + 0.89D_p - 8084 \quad (13)$$

With $R^2 = 83.39\%$

The R^2 value signifies the goodness of the regression equation compared to the simulated/actual value. R^2 Value for pressure drop achieved from linear regression analysis is not good enough to be used as predictive model equation. Hence this regression equation has been modified adopting the 2nd order multi-regression analysis. The obtained equation is represented as follows

$$\frac{\Delta P}{L} = 582.473403V_m - 11293.3395C_{vf} - 30.3219765D_p - 2865.31176V_m \times C_{vf} + 337.913053C_v \times D_p + 36.2469524V_m \times D_p - 273.246176{V_m}^2 - 1.02945031{D_p}^2 - 195.066387 \quad (14)$$

With $R^2 = 99.9991\%$

Figures 15 and 16 shows the goodness of the fit for predictive model equation of particle flow velocity and pressure drop respectively.

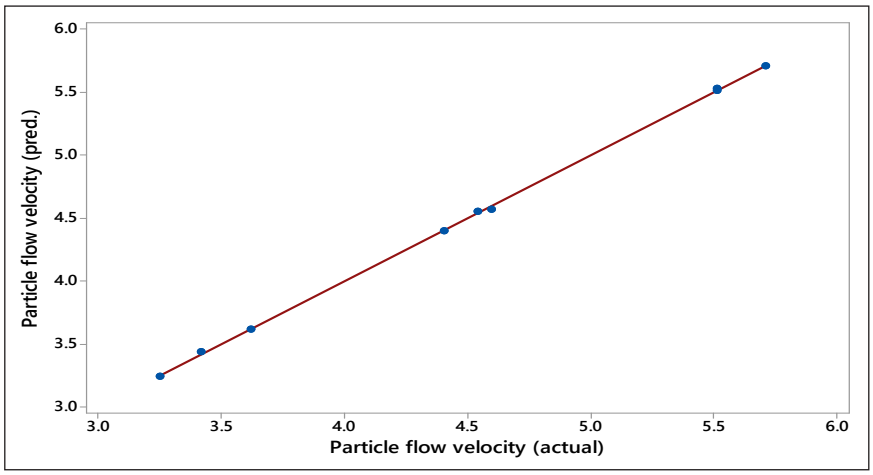

Figure 15. Regression plot of particle flow velocity (predicted) vs. Particle flow velocity (simulated)

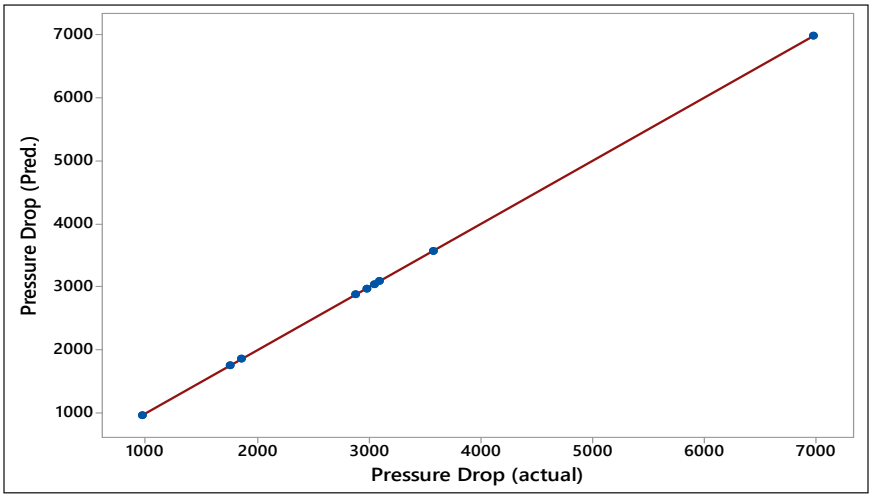

Figure 16. Regression plot of particle flow velocity (predicted) vs. Particle flow velocity (simulated)

From Figures 15 and 16 it can be noticed that the responses obtained from regression model equations for particle flow velocity and pressure drop shows a well aligned nature with the simulation data. Hence a predictive model consisting of these two equations can predict the particle flow velocity and pressure drop with minimal error (of the order of 0.001%).

Validation of the Developed Mathematical Model

The outcome obtained from the predictive mathematical model show a good reliability with the simulated results. In addition, to establish the robustness and reliability of this proposed model these outcomes have been compared with the experimental data taken from the work of Kaushal and Tomita (2007) and recorded in Table 8.

Table 8
Comparison of simulated and experimental responses with the proposed predictive mathematical model

	Flow Parameter combination			Responses	
	V_m (m/s)	C_{vf}	D_p (μm)	V_f (m/s)	$\frac{\Delta P}{L}$ (Pa/m)
Predicted by Proposed model	3	0.4	125	3.43902	1750.28
	4	0.3	125	4.39619	1856.32
	5	0.5	125	5.70786	6974.70
Experimental (Kaushal and Tomita ,2007)	3	0.4	125	-	1913.6
	4	0.3	125	-	2088.69
	5	0.5	125	-	6887.58
Simulated	3	0.4	125	3.418	1750.23
	4	0.3	125	4.403	1856.27
	5	0.5	125	5.712	6974.65

From Table 8 it can be observed that the predicted outcomes of the mathematical model are reliable and show excellent consistency with the experimental data. This model can predict the pressure drop data with an average error of 6.95% when compared with experimental data.

Multi-Objective Optimization of Particle Flow Velocity and Pressure Drop using Genetic Algorithm

Genetic algorithm (GA) is an artificially intelligent evolutionary algorithm which is capable of optimizing single objective as well as multiple objectives (responses) for various control variables within a specific range. GA is often preferred for optimizing multi-objective problem because it yields more accurate and effective outcome compared to other evolutionary algorithm (Oktem, 2009). GA is inspired by the biological evaluation process: Darwin's theory of survival for the fittest. The optimization process is initiated generating random potential solutions known as *'chromosomes'*. The whole set of chromosomes create a "*population"*. Chromosomes evolve in the process of several iterations known as '*generation.*' New offspring are evaluated by the process of '*crossover'* and '*mutation'*. Crossover divides each chromosome into two parts and combines one half with other half of a different chromosome. While mutation flips over a single chromosome. Chromosomes are then evolved with the usage of specific fitness criteria and best chromosomes remains in the solution while the rest are discarded. This process keeps repeating until at least one chromosome is evolved which possesses the quality of best fitness and it is considered as optimal solution.

Finding a specific combination of process variables which would maximize the particle flow velocity and reduce the pressure drop simultaneously is necessary in order to initiate a smooth slurry flow through the selected pipe section which would yield maximum transport efficiency. The optimal combination of process variables obtained from S/N ratio analysis can minimize only one response at a time (Table 6). Specific combination of control factors can be achieved within the range of optimal control factors enlisted in Table 6 with the help of Multi-objective GA optimization technique.

Chosen Objectives

The objective functions chosen are as under:

$$V_f = 1.07533V_m + 1.1817C_{vf} + 0.002307D_p - 0.5481 \quad (15)$$

$$\frac{\Delta P}{L} = 582.473403V_m - 11293.3395C_{vf} - 30.3219765D_p - 2865.31176V_m \times C_{vf} + 337.913053C_{vf} \times D_p + 36.2469524V_m \times D_p - 273.246176{V_m}^2 - 1.02945031{D_p}^2 - 195.066387 \quad (16)$$

Design/Decision Variables

The design parameters chosen in this present work are as under:

- Inlet mean velocity V_m in m/s
- Solid Volume Fraction C_{vf}
- Particle size D_p in μm

Constraints

The ranges for these variables are given as under:

$$4\text{m/s} \leq \text{V}_\text{m} \leq 5\text{m/s}$$

$$0.4 \leq \text{C}_\text{vf} \leq 0.5$$

$$125\ \mu\text{m} \leq \text{D}_\text{p} \leq 150\ \mu\text{m}$$

Fitness function was created from equation 16 and 17 using MATLAB and codes were written accordingly. The following genetic algorithm critical factors are used in this proposed research work

Population type: Double vector
Population size: 50
Creation function: feasible population
Tournament size: 2
Mutation: Adaptive feasible
Crossover: Constraint dependent (ratio 1.0)
Maximum number of generations: 1000

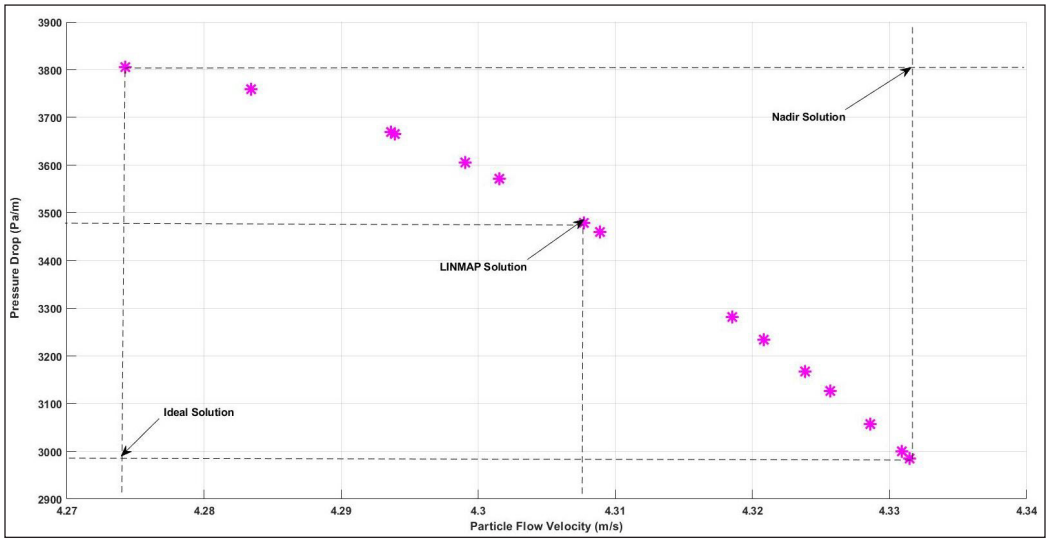

Figure 17. Plot of Pareto optimal solution for Particle flow velocity and Pressure drop obtained from GA optimization

In multi-objective optimization problem, a typical pareto frontier is attained and a final outcome from pareto set is obtained by suitable decision-making approach. It is presented in Figure 17. In the present study, the aim is to achieve minimum pressure drop for maximizing the particle flow velocity in order to encounter a smooth slurry flow process. All the values in the pareto front represent optimal values and hence, LINMAP method was employed for getting optimum solution of aforesaid objectives from pareto front. In case of LINMAP method the magnitude of distance between ideal/nadir points and the position of each individual was evaluated by distance matrices called Euclidian distance which is evaluated as below:

$$D_{i+} = \sqrt{\sum_{j=1}^{n} \left(F_{ij} - F_j^{ideal}\right)^2} \qquad (17)$$

LINMAP approach evaluates the minimum distance with respect to ideal value as follows:

$$i_f = i \in \min\left(D_{i+}\right) \qquad (18)$$

Employing this approach, the optimal value of Particle flow velocity (V_f) and pressure drop ($\frac{\Delta P}{L}$) are found to be 4.309 m/s and 3460.108 Pa/m respectively. A specific combination of process variables can be obtained at this optimal point as:

- V_m = 4 m/s
- C_{vf} = 0.4
- D_p = 140.002 μm

In other words, using a combination of inlet mean velocity of 4 m/s, solid volume fraction of 0.4 and particle size of 140.002 μm optimal particle flow velocity of 4.309 m/s and pressure drop of 3460.108 Pa/m can be acquired in a Glass-water slurry flow through 4 m long and 54.9 mm diameter horizontal pipe. This optimal condition can be used for optimal design of the pipeline and to encounter a smooth slurry flow through horizontal pipeline.

Validation of GA Optimized Results with Simulated Results

The simulated results show excellent consistency with the experimental data taken from the work of Kaushal and Tomita (2007). Hence the reliability of GA analysis has been carried out comparing the outcome obtained from GA analysis with the CFD simulated results. The specific combination of input parameters obtained from GA analysis (V_m = 4 m/s, C_{vf} = 0.4 and D_p = 140.002 μm) was used in CFD simulation and the outcomes are recorded in Table 8.

Table 9
Comparison of responses obtained from GA optimization strategy with CFD simulation results

	Optimal Input Parameters			Responses	
	Inlet Mean Velocity (m/s)	Solid Volume fraction	Particle Size (μm)	Particle Flow Velocity (m/s)	Pressure Drop (Pa/m)
GA Optimized	4	4	140.002	4.309	3460.108
Simulated	4	4	140.002	4.597	3392.5

The recorded data in Table 9 show that the GA optimized results are in excellent consistency with the CFD simulated results with mean percentage error of 4.13%. Hence this new strategy can be used to optimize multiple responses simultaneously in a complex multiphase slurry flow problem considering a range of flow parameters.

Reduction in Pressure Drop Implementing the GA Optimization Strategy

The optimal combination of flow parameters for individual optimization of particle flow velocity and pressure drop was attained from S/N ratio analysis while designing the experiments using Taguchi's method (Table 7). The combination is essential in order to have a primary idea about the ranges of flow parameters that would yield optimal responses in GA analysis. From Table 7 the mean optimal particle flow velocity and mean optimal pressure drop was calculated to be 5.084 m/s and 4902.9775 Pa/m. These responses had been compared with the outcome of GA analysis (Table 9) in order to find the % increase in particle flow velocity and % reduction in pressure drop as follows:

$$\%\ \text{increase in Particle flow velocity} = \frac{V_{f(\text{Taguchi})} - V_{f(\text{GA})}}{V_{f(\text{Taguchi})}} \times 100\%$$

$$\frac{5.084 - 4.309}{5.084} \times 100\% = 15.24\%$$

$$\%\ \text{Reduction in Pressure Drop} = \frac{\frac{\Delta P}{L}_{(Taguchi)} - \frac{\Delta P}{L}_{(GA)}}{\frac{\Delta P}{L}_{(Taguchi)}} \times 100\%$$

$$\frac{4902.9775 - 3460.108}{4902.9775} \times 100\% = 29.42\%$$

Hence after implementing the GA approach and using the specific flow conditions obtained from GA analysis 15.24% increase in particle flow velocity and 29.42% reduction in pressure drop can be observed over the responses obtained from Taguchi's method and S/N ratio analysis.

Validation of the Study

The aim of this section is to legitimize the simulated results of pressure drop obtained from CFD analysis with the experimental results of pressure drop available in the previous literature (Kaushal and Tomita, 2007). The Figures 18 to 20 show the plot of simulated pressure drop and the experimental pressure drop at 0.3, 0.4 and 0.5 volume fraction for a particle size of 125µm respectively.

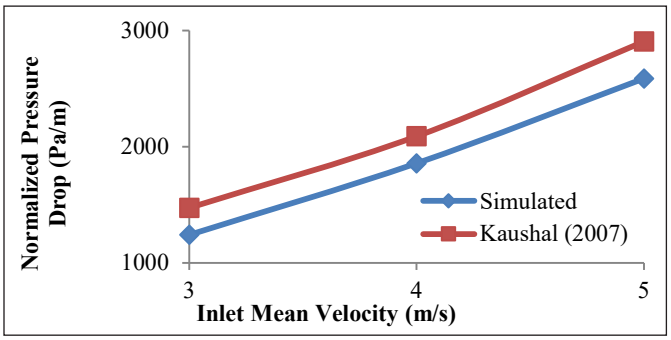

Figure 18. Comparison of simulated and experimental pressure drop at 0.3 solid volume fraction for 125µm particle size

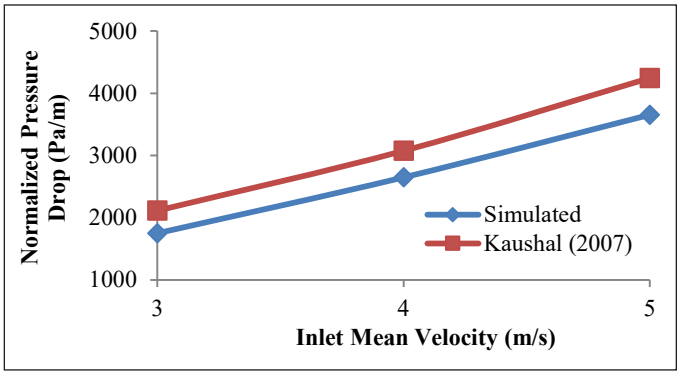

Figure 19. Comparison of simulated and experimental pressure drop at 0.4 solid volume fraction for 125µm particle size

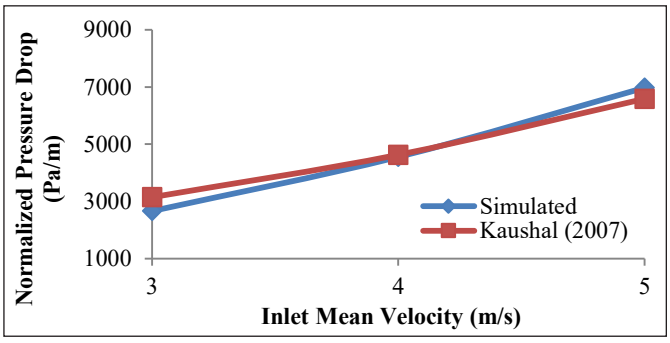

Figure 20. Comparison of simulated and experimental pressure drop at 0.5 solid volume fraction for 125µm particle size

CONCLUSION

This study represents an Eulerian two phase glass beads water slurry flow considering three different glass beads (specific gravity 2.47) particle size viz. 90µm, 125µm and 150µm through a horizontal pipe of 4m long and 54.9 mm diameter. The flow simulations are conducted at three different inlet mean velocities viz. 3m/s, 4m/s and 5m/s along with three different solid volume fraction viz. 0.3, 0.4 and 0.5 by volume. In this study the influence of various flow variables on pressure drop has been analysed as well as optimum flow conditions for smooth slurry flow has been analysed using Taguchi's decision-making technique and ANOVA. Multi-objective optimization of the responses have been undertaken in order to optimize both the responses simultaneously for a specific combination of flow parameters. Based on this study the following conclusions can be drawn:

- For all particle size the particle flow velocity distribution is asymmetrical at the lower part of the pipe at low inlet mean velocities. However, as the mean velocity increases the particle flow velocity distribution becomes less asymmetrical.
- At a constant inlet mean velocity the particle flow velocity increases as the solid volumetric concentration of the particles in the slurry becomes higher. Furthermore, the simulated results showed that the maximum concentration at the pipe bottom for 90µm is 0.35 whereas for 150µm particles it goes up to 0.41.
- The particle flow velocity is low for the smaller particle size and it increases as the particle size becomes larger.
- The solid particles are heterogeneously distributed in the fluid establishing a high accumulation zone at the base of the pipe; it can be observed that the solid particles gravitate at the bottom of the pipe when the inlet mean velocity is less, however when the mean velocity increases the solid particles become more buoyant in the fluid rather than settling down at the pipe bottom. Furthermore, the smaller particles are more homogenously distributed in the fluid than the larger particles because the larger particles tend to settle down at pipe bottom due to gravitational effect thereby forming a moving bed at lowest part of the pipe.
- Pressure drop increases with the increase in inlet mean velocity; because with the increase in mean velocity there in an increase in turbulence in the flow. Moreover, the pressure drop becomes higher when the solid volume fraction and particle size increases.
- From the S/N Ratio analysis of Taguchi's method optimal combinations of flow parameters have been achieved in order to optimize particle flow velocity and pressure drop individually.
- From ANOVA analysis it can be determined that for maximum particle flow velocity which is the desirable condition for smooth slurry flow and better productivity; the most influencing flow parameter is inlet mean velocity (contribution=98.38%)

followed by solid volume fraction (contribution=1.19%) and particle size (contribution=0.02%). For nominal pressure drop the most influencing flow parameter is found to be the solid volume fraction (contribution=48.41%) followed by inlet mean velocity (contribution=39.6%) and particle size (contribution=5.31%).

- A mathematical predictive model has been proposed for envisaging the responses analytically and it has been concluded that the proposed model can predict the responses with 6.95% error when compared to the experimental results.
- Genetic Algorithm has been coupled with the outcome of Taguchi's method in order to deal with the multi-objective optimization problem and a specific combination of flow parameters have been attained which can optimize the particle flow velocity and pressure drop simultaneously. The outcome of GA analysis has been compared with the simulated results and can be concluded that this strategy is efficient for optimizing multiple responses in a complex multiphase slurry flow problem. In addition it may be concluded that adopting this new GA approach particle flow velocity can be increased by 15% and pressure drop can be reduced by 29%.

The proposed mathematical model and outcomes of this current study can be applied for future academic research as well as in thermal power plants, food processing industries, chemical and pharmaceutical industries, slurry transporting industries and Oil and Gas industries in order to obtain an optimal pipe design. Further this new integrated Taguchi-GA approach would be helpful for optimizing pressure drop and particle flow velocity thereby initiating a smooth slurry flow which would reduce the power consumption/energy requirements as well as improve the transport efficiency in a complex multiphase slurry flow through horizontal pipelines.

ACKNOWLEDGEMENT

The authors would like to thank Amity University Haryana, India for providing support in carrying out this valuable research work.

REFERENCES

Chandel, S., Singh, S. N., & Seshadri, V. (2010). Transportation of high concentration coal ash slurries through pipelines. *International Archive of Applied Sciences and Technology*, *1*, 1-9.

Doron, P., Granica, D., &Barnea, D. (1987). Slurry flow in horizontal pipes-experimental and modeling. *International Journal of Multiphase Flow, 13*(4), 535-547.

Gillies, R. G., Shook, C. A., & Wilson, K. C. (1991). An improved two layer model for horizontal slurry pipeline flow. *The Canadian Journal of Chemical Engineering, 69*(1), 173-178.

Gillies, R. G., Shook, C. A., & Xu, J. (2004). Modelling heterogeneous slurry flows at high velocities. *The Canadian Journal of Chemical Engineering, 82*(5), 1060-1065.

Kaushal, D. R., & Tomita, Y. (2007). Experimental investigation for near-wall lift of coarser particles in slurry pipeline using γ-ray densitometer. *Powder Technology, 172*(3), 177-187.

Kaushal, D. R., Thinglas, T., Tomita, Y, Kuchii S., & Tsukamoto, H. (2012). CFD modeling for pipeline flow of fine particles at high concentration. *International Journal of Multiphase Flow, 43*, 85-100.

Kotcioglu, I., Cansiz, A., & Khalaji, M. N. (2013). Experimental investigation for optimization of design parameters in a rectangular duct with plate-fins heat exchanger by Taguchi method. *Applied Thermal Engineering*, *50*(1), 604-613.

Lahiri, K. S., & Ghanta, K. C. (2010). Slurry flow modelling by CFD. *Chemical Industry and Chemical Engineering Quarterly, 16*(4), 295-308.

O'Brien, M. P. (1933). Review of the theory of turbulent flow and its relations to sediment transport. *Transaction of the American Geophysical Union, 14*, 487-491.

Öktem, H., (2009). An integrated study of surface roughness for modelling and optimization of cutting parameters during end milling operation. *International Journal of Advance Manufacturing and Technology, 43*(9-10), 852-861.

Oroskar, A. R., & Turian, R. M. (1980). The critical velocity in pipeline flow of slurries. *American Institute of Chemical Engineers Journal*, *26*(4), 550-558.

Roco, M. C., & Shook, C. A. (1983). Modeling of slurry flow: the effect of particle size. *The Canadian Journal of Chemical Engineering*, *61*(4), 494-503.

Rouse, H. (1937). Modern conceptions of the mechanics of fluid turbulence. *American Society of Civil Engineers*, *102*, 463-505.

Toda, M., Ishikawa, T., Saito, S., & Maeda, S. (1973). On the particle velocities in solid-liquid two-phase flow through straight pipes and bends. *Journal of Chemical Engineering of Japan*, *6*(2), 140-146.

Turian, R. M., & Yuan, T. F. (1977). Flow of slurries in pipelines. *AIChE Journal, 23*(3), 232-243.

Wu, S. J., Ouyang, K., & Shiah, S. W. (2008). Robust design of microbubble drag reduction in a channel flow using the Taguchi method. *Ocean Engineering*, *35*(8-9), 856-863.